

Supporting Information

Smooth, Transparent and Nonperfluorinated Surfaces Exhibiting Unusual Contact Angle Behavior Toward Organic Liquids

Chihiro Urata, Dalton F. Cheng, Benjamin Masheder and Atsushi Hozumi*

National Institute of Advanced Industrial Science and Technology (AIST),
2266-98, Anagahora, Shimoshidami, Moriyama, Nagoya 463-8560, Japan

Materials and Methods

Materials

Ethanol, 0.01M HCl, diiodomethane, oleic acid, soybean oil, toluene, *p*-xylene, *n*-hexadecane, turpentine oil, *n*-dodecane, and *n*-decane were purchased from Wako Pure Chemical Industries Ltd. Sudan III and tetramethoxysilane (TMOS) were purchased from Tokyo Kasei Kogyo. Co., Ltd. Decyltriethoxysilane (DTES) was purchased from Gelest Inc. Ethanol-*d* and D₂O were purchased from Cambridge Isotope Laboratories Inc. Blue food color (spirulina dye) was purchased from Watashinodaidokoro Inc. All chemicals were used as received.

Sample preparation

Our hybrid films contain decylsilyl groups (C₁₀-hybrid films) and were prepared using conventional co-hydrolysis and co-condensation according to a previously reported method.¹

(1) Preparation of siloxane-organic hybrid (C₁₀-hybrid) films

C₁₀-hybrid films were prepared by a simple sol-gel and subsequent coating process. Mixed solution of DTES and TMOS were co-hydrolysed and co-condensed in an ethanol/hydrochloric acid solution for 24 h at 25 ± 2 °C. The molar ratio of the reaction mixture was DTES/TMOS/EtOH/H₂O/HCl = 1:X:50:22:4×10⁻⁴, where X is 0, 1, 2, 3, 4, 5, 6, 7, 8, 9, 10. For NMR measurement, ethanol-*d* and D₂O were used instead of ethanol and H₂O. Under these experimental conditions, complete hydrolysis of both

alkoxysilanes were observed by nuclear magnetic resonance (NMR) spectroscopy (data not shown). The precursor solutions were then spincoated onto UV/ozone-cleaned glass, Si or polymer (polycarbonate (PC) and poly(methyl methacrylate) (PMMA)) substrates ($24 \times 48 \text{ mm}^2$) at 500 rpm for 5 s and 1000 rpm for 10 s at $25 \pm 2^\circ\text{C}$ and under relative humidity of $40 \pm 5\%$. For IR measurements and SEM observations, the precursor solutions were spincoated onto one side of double-sided polished silicon wafers. For liquid transportation experiments, the glass tube ($200 \text{ mm} \times \varphi_{\text{outside}} 6.1 \text{ mm} \times \varphi_{\text{inside}} 3.5 \text{ mm}$) was dipped into the precursor solution (TMOS/DTES ($R_{\text{T/D}}$) = 4), pulled out at a speed of 60 mm/min (at room temperature, $25 \pm 2^\circ\text{C}$, and relative humidity of $40 \pm 5\%$), and dried in air for more than 24 h.

(2) Preparation of decylsilyl monolayer (C₁₀-monolayer)

A C₁₀-monolayer was prepared on UV-ozone cleaned glass slides, UV-activated PC, or PMMA substrates by chemical vapor deposition (CVD) method. Each of the substrates ($24 \times 48 \text{ mm}^2$) were placed, together with a small glass vial containing 20 μL of DTES, into a 60 cm^3 Teflon® container in a dry N₂ atmosphere. The container was sealed with a cap and then heated for 72 h at 100°C in an oven. Individual samples were rinsed with hexane and water, in that order, and then blown dry with a N₂ stream. For ellipsometry measurements, C₁₀-monolayers were prepared on one side of double-sided polished silicon wafers. For liquid transportation experiments, C₁₀-monolayers were also fabricated inside the glass tube in the same manner.

(3) Transportation experiments of liquids

- i) Red-colored *n*-hexadecane (0.50 mL) was poured into vertically-fixed C₁₀-hybrid ($R_{\text{T/D}}=4$)- and C₁₀-monolayer-coated glass tubes.
- ii) Blue-colored water and red-colored *n*-hexadecane (0.50 mL) were flowed into the C₁₀-hybrid ($R_{\text{T/D}}=4$)-coated glass tubes in which one side was plugged with a paraffin film.

Characterization

Liquid-state ²⁹Si nuclear magnetic resonance (NMR) spectra were recorded on a JEOL Lambda-500 spectrometer at a resonance frequency of 500 MHz with a pulse width of 6.5 μs and recycle delay of 10 s. The solution was placed in a 5 mm diameter glass tube, where ethanol-*d* and D₂O were used for obtaining a lock signal. Cr(acac) was added to reduce the ²⁹Si spin-lattice relaxation time. Chemical shifts were

referenced to tetramethylsilane at 0 ppm. X-ray diffraction (XRD) patterns were obtained by using Rigaku RINT 2100 diffractometer with monochromated Fe-K α radiation. Hardness of hybrid films were estimated by using a home-made instrumented indentation microscope according to a previous report. Field emission scanning electron microscope (FE-SEM) images were obtained by JSM-7100F (JEOL). In order to place emphasis on the surface roughness of the hybrid films, the samples were tilted at 45° during the observation. We intentionally centered microscopy on contaminant particles in the hybrid surface for the purpose of focusing on the surface under the observation. Film thicknesses of C₁₀-hybrid films were measured by a stylus profiler (Veeco Dektak 6M). Contact angles (CAs) were measured with a CA goniometer (Kyowa Interface Science CA-V150). The CAs were collected using several probe liquids (water, diiodomethane, oleic acid, soybean oil, toluene, *p*-xylene, *n*-hexadecane, turpentine oil, *n*-dodecane, *n*-decane, and ethanol) at room temperature (25 °C). For static (θ_S) CA measurement, probe liquids (about 3 μ L) were placed gently on the samples. For dynamic (advancing (θ_A) and receding (θ_R) CA measurement, probe liquid droplets (about 3 μ L) were added and withdrawn from the surface, respectively. Measurements were taken at three different locations on each sample surface. The CA data reported here was determined by averaging the averaged values of three samples (n=3) which were prepared in independent experiments. Minimum tilt angles needed to set probe liquid droplets (5 μ L) in motion on the samples were measured using a custom-made tilt angle meter. Thickness of C₁₀-monolayer was determined by ellipsometry (Philips, PZ2000) equipped with a He-Ne laser (632.8 nm) with its incident angle fixed at 70°. The morphology of the samples was observed by atomic force microscope (AFM, XE-100, Park Systems) using a Si probe (Park Systems, 910M-NCHR; spring constant = 42 N/m and response frequency of 330 kHz) in non-tapping mode. X-ray photoelectron spectroscopy (XPS, Shimadzu, ESCA3400) was performed using MgK α radiation. The X-ray source was operated at 20 mA and 12 kV. The photoelectron take-off angle was set at 90°. Fourier-transformed infrared (FT-IR, Agilent, Digilab FTS-7000) spectra were recorded at a resolution of 4 cm⁻¹ for 256 scans. Images in Figure 1-b, -c, and Figure 2 were obtained by capturing still images from Movie S1-4.

Table S1. CA data for C₁₀-monolayer-covered surfaces reported in the literature.

Substrate	Chemical	Reaction condition	$\theta_A / \theta_R / \Delta\theta$ (°/°/°) Water	$\theta_A / \theta_R / \Delta\theta$ (°/°/°) <i>n</i> -Hexadecane	Ref
Si wafer ^a	CH ₃ (CH ₂) ₉ Si(CH ₃) ₂ Cl	Liquid phase	104/92/12	9/<5/>4	
		Vapor phase	106/95/11	11/6/5	
	CH ₃ (CH ₂) ₉ Si(CH ₃)Cl ₂	Liquid phase	104/92/12	12/7/5	Fadeev et al. ²
		Vapor phase	107/100/7	14/7/7	
	CH ₃ (CH ₂) ₉ SiCl ₃	Liquid phase	106/92/14	15/5/10	
		Vapor phase	110/100/10	16/6/10	
Au ^b	CH ₃ (CH ₂) ₉ SH		111/102/9	46/40/6	
	CH ₃ (CH ₂) ₇ CH(CH ₂ SH) ₂	Liquid phase	101/90/11	16/-/-	Park et al. ³
	CH ₃ (CH ₂) ₇ C(CH ₃)(CH ₂ SH) ₂		98/88/10	-/-/-	
Al alloy ^a (2024-T3)	CH ₃ (CH ₂) ₉ Si(OCH ₂ CH ₃) ₃	Liquid phase	117/49/68	N/D ^c	Hintze et al. ⁴

(a): Surfaces are oxidized, (b): Gold coated silicon wafer, (-): Less than 10°, (c): no date

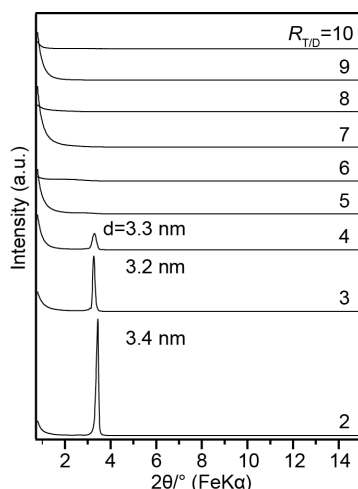


Figure S1. XRD patterns of C₁₀-hybrid films prepared at different $R_{T/D}$ ratios.

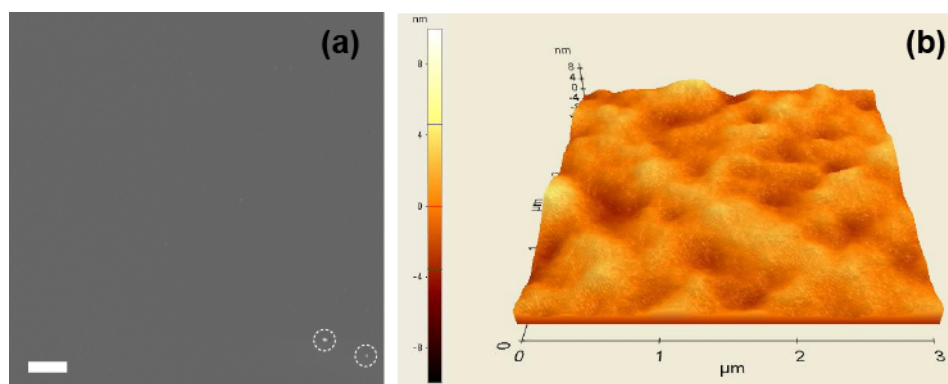
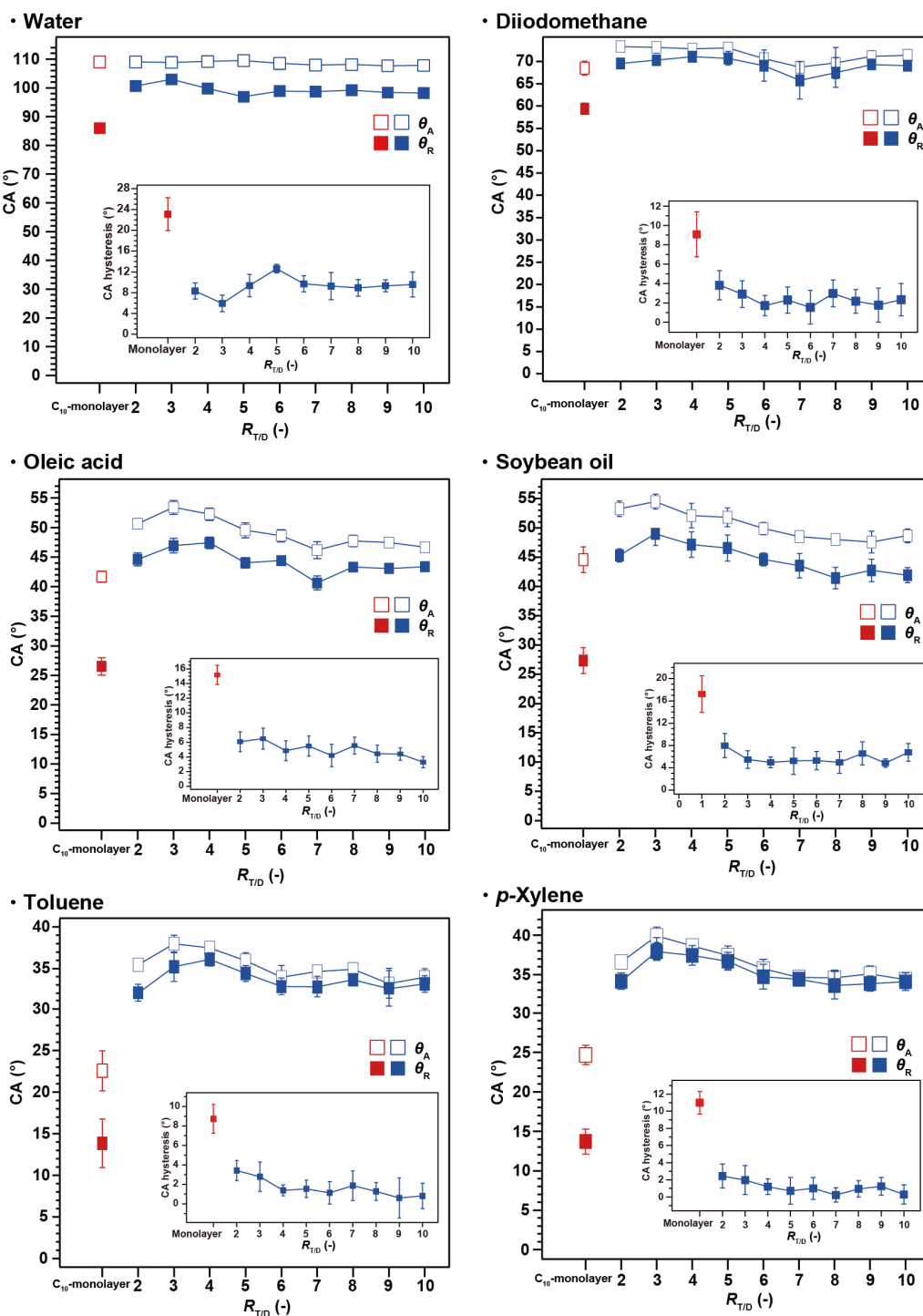


Figure S2. (a) Typical SEM (scale bar = 10 μ m) and (b) AFM images (root-mean-square roughness (R_{rms}) = 1.1 nm) of C₁₀-hybrid film ($R_{T/D} = 4$). Dashed open circles in SEM image show the impurity particles on the hybrid surface.



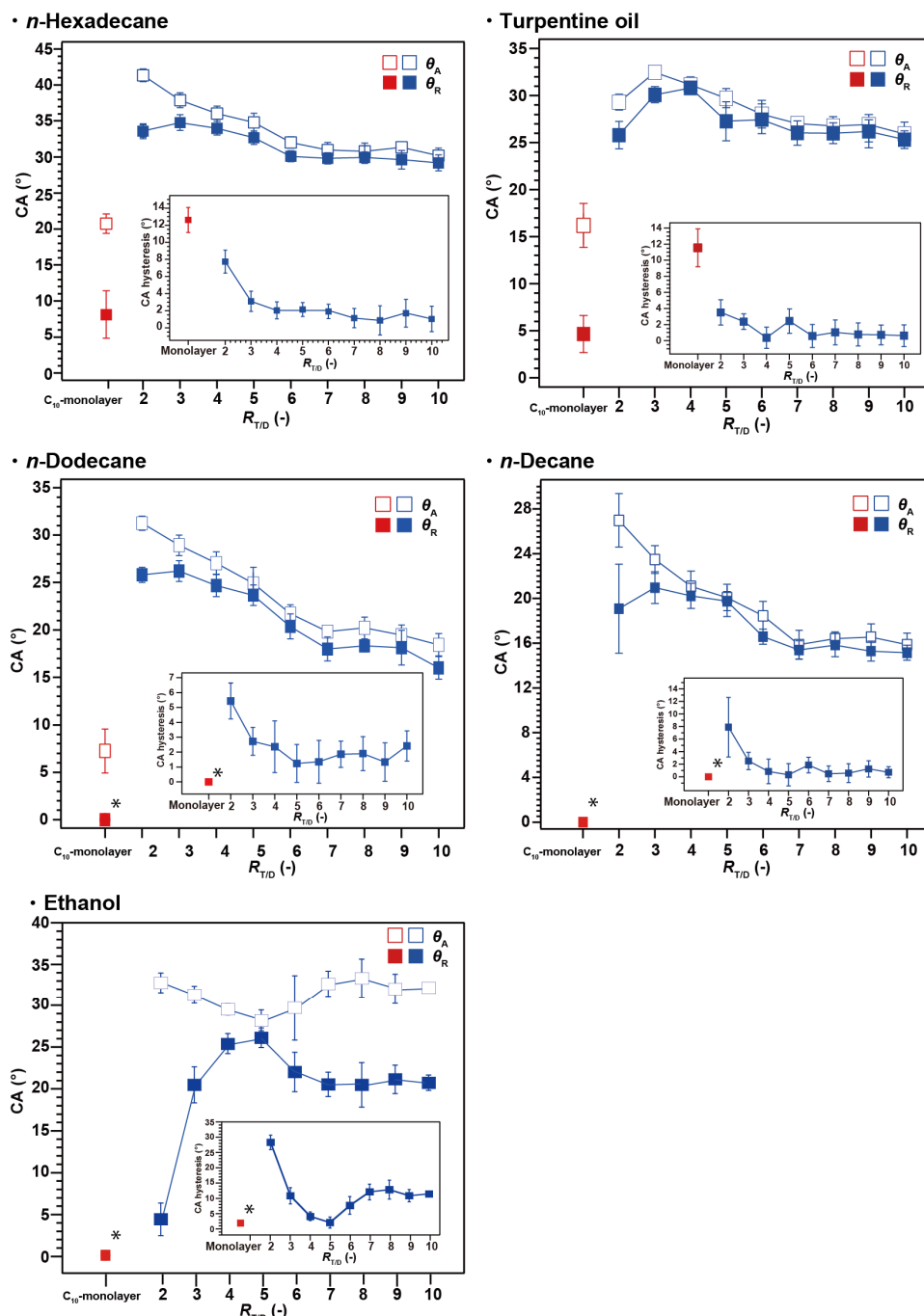


Figure S3. Dynamic CAs and CA hysteresis (inset) of C_{10} -monolayer- and C_{10} -hybrid-covered samples. Data represent the mean \pm standard deviation from three independent experiments. ($n=3$)

* We could hardly measure the θ_R of *n*-dodecane and θ_A and θ_R of *n*-decane and ethanol because of complete wetting.

In order to confirm the versatility of our coating method, C₁₀-hybrid films and C₁₀-monolayers were formed on PC and PMMA substrates. In the latter case, polymer surfaces were preliminarily activated by 172 nm vacuum UV light before coating. As shown in Figure S6 -a, -b, -d, and -e, transparency and appearance of these polymer substrates remained intact even after the C₁₀-hybrid coating. The C₁₀-hybrid coated polymer substrates also exhibited excellent dynamic dewetting behaviour similar to that of the C₁₀-hybrid on the glass substrates (Table S2). In contrast, the monolayer-covered polymer substrates were discoloured and considerably deformed (Figure S6 c and f) due to the thermal stress and/or infiltration of C₁₀-TES into polymer substrates. Their final surface dewettability was found to be inferior to that of C₁₀-hybrid-covered polymer substrates.

This is a clear advantage offered by our sol-gel coating process being conducted at room temperature.

Table S2. θ_A , θ_R , and $\Delta\theta$ values of water (upper (gray) row) and *n*-hexadecane (lower (lighter) row) on PC and PMMA substrates before and after coating of C₁₀-hybrid films and C₁₀-monolayers.

Coating method	Substrate	Before coating		After coating	
		θ_A/θ_R (%)	$\Delta\theta$ (°)	θ_A/θ_R (%)	$\Delta\theta$ (°)
Sol-gel method	PC	93/76	17	108/100	8
		8/-	>8	34/33	1
	PMMA	63/55	8	111/100	11
		-/-	-	39/37	2
CVD method	PC	50/-	>50	130/67	63
		-/-	-	7/-	>7
	PMMA	42/-	>42	N/A	N/A
		-/-	-/-	N/A	N/A

(N/A: Because of the deformation of PMMA after CVD treatment, CA could not be measured.)

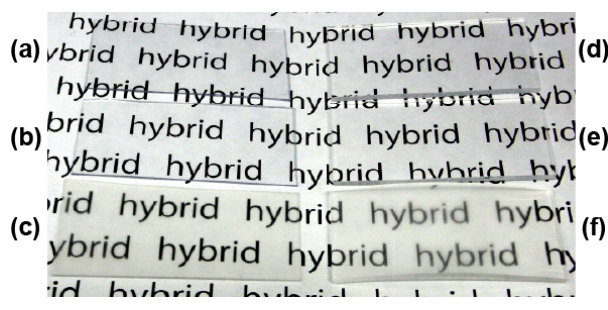


Figure S4. Appearances of PC (a-c) and PMMA (d-f) substrates before (a,d) and after C₁₀-hybrid film (b, e) and C₁₀-monolayer (c, f) formation.

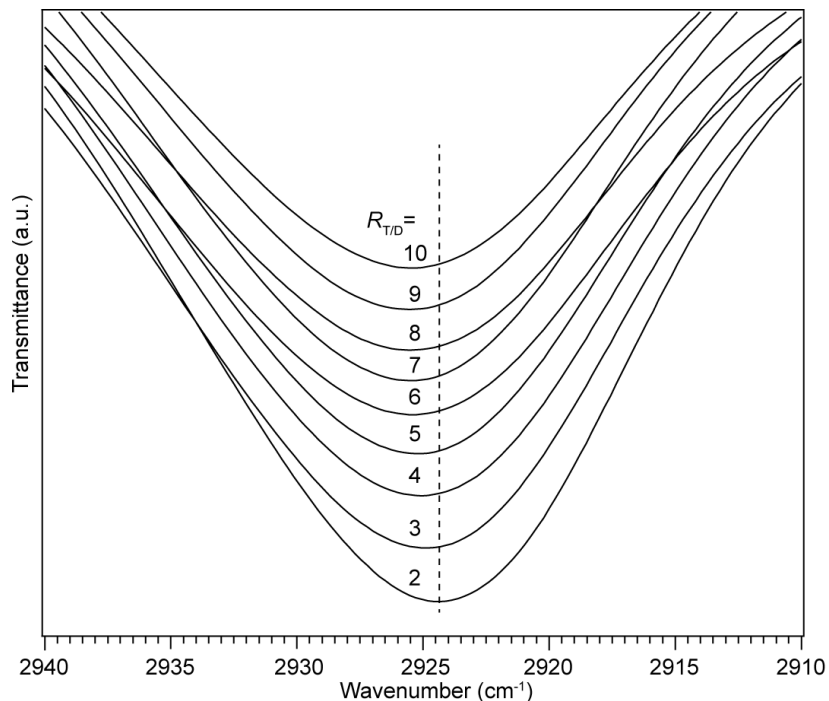


Figure S5. IR spectra (CH₂ asymmetric (ν_{as}) vibration) of the C₁₀-hybrid films prepared at different $R_{T/D}$ ratios (Dashed line indicates the peak top of the spectrum for $R_{T/D}=2$).

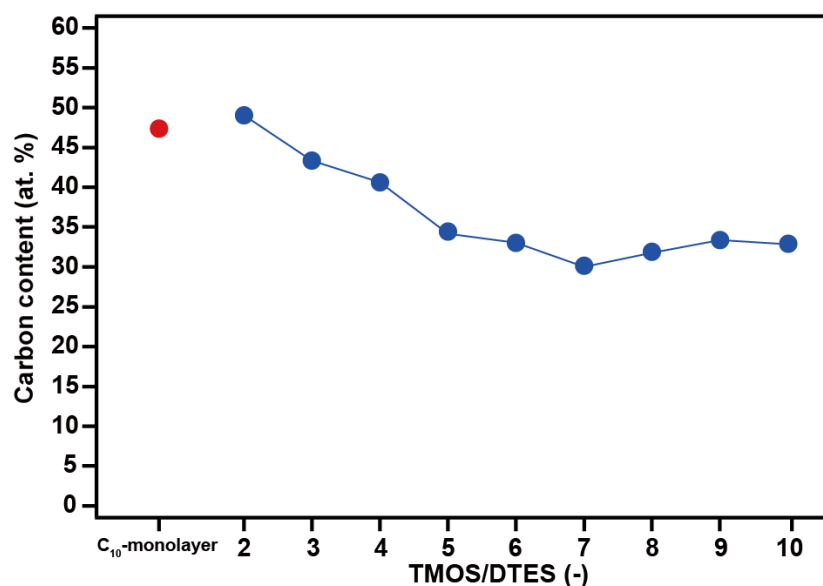


Figure S6. Carbon (C) concentrations in the C₁₀-hybrid films as a function of $R_{T/D}$ ratio (For comparison, C concentration in the C₁₀-monolayer-covered glass surface was indicated by the red-solid-circle).

Movie S1. Spray test using a mist of red-colored *n*-hexadecane on the C₁₀-hybrid- ($R_{T/D}=4$) and C₁₀-monolayer-covered glass surfaces.

Movie S2. Transportation of red-colored *n*-hexadecane within the C₁₀-hybrid ($R_{T/D}=4$)- and C₁₀-monolayer-coated glass tubes.

Movie S3. Transportation of blue-colored water within the C₁₀-hybrid ($R_{T/D}=4$)-coated glass tube in which one end was plugged by a paraffin film.

Movie S4. Transportation of red-colored *n*-hexadecane within the C₁₀-hybrid ($R_{T/D}=4$) - coated glass tube in which one end was plugged by a paraffin film.

References

1. Shimojima *et al.*, *J. Am. Chem. Soc.*, **120**, 4528 (1998); *Chem. Mater.*, **13**, 3610 (2001); *Langmuir*, **18**, 1144 (2002); *J. Organomet. Chem.*, **686**, 223 (2003).
2. Fadeev *et al.*, *Langmuir*, **16**, 7268, (2000).
3. Park *et al.*, *Langmuir*, **20**, 5829 (2004).
4. Hintze *et al.*, *Electrochim. Acta.*, **51**, 1761 (2006).